



Research Article

ACTIVATION PARAMETERS AND ADSORPTION BEHAVIOR OF 1-ISONICOTINOYL-4-PYRIDIN-2-YL PIPERAZINE ON MILD STEEL IN ACID ENVIRONMENT

Sumathi P^{1*}, Kannan K²

¹Department of Chemistry, Knowledge Institute of Technology, Salem, Tamilnadu, India

²Department of Chemistry, Government College of Engineering, Salem, Tamilnadu, India

*Corresponding Author Email: sumathi.murugan25@gmail.com

Article Received on: 10/03/17 Approved for publication: 23/04/17

DOI: 10.7897/2230-8407.080453

ABSTRACT

The adsorptions 1-isonicotinoyl-4-pyridin-2-ylpiperazine on metal surface was studied at various temperatures (303K-333K) were found to obey Langmuir adsorption isotherm. Temperature study was carried out and thermodynamic parameters and the physical adsorption is proposed from the values of (E_a , ΔG_{ads} and K_{ads}) were also determined. AFM and FT-IR studies clearly reveal the formation of an inhibitor molecules strongly adsorbed on to the surface.

Keywords: Adsorption, Temperature, Activation parameters, AFM, FT-IR

INTRODUCTION

The most important fields of application being acid pickling, industrial acid cleaning, acid descaling and oil well acidizing, because of the general aggressiveness of acid solutions, Process of corrosion depend upon aggressiveness of the medium and reactivity of the material. In many industries (especially chemical industry) mineral acids are frequently used in various applications which cause loss of functional properties of the metals, in form of corrosion, due to violent reaction of acid with metals¹. The practice of inhibition is commonly used to reduce the corrosive attack on metallic materials. Most corrosion inhibitors for mild steel in acidic medium are organic compounds containing nitrogen, oxygen and/or sulfur²⁻⁵. In many cases, organic inhibitors (chemically synthesized) were found very efficient but its toxicity and synthesis cost motivated people to develop environment friendly and cheap inhibitors. In the present investigations, new synthesized 1-isonicotinoyl-4-pyridin-2-yl piperazine (ICPP) by using 1-(pyridin-2-yl) piperazine as parent moiety and adsorption behavior, activation parameters. Surface morphology was studied by using adsorption calculations, FT-IR and AFM.

MATERIALS AND METHODS

Mild steel specimens of the following composition were used for the corrosion studies. Iron-99.686%, Nickel-0.013%, Molybdenum-0.015%, Chromium-0.043%, Sulphur-0.014%, Silicon-0.007%, Manganese-0.196%, Carbon-0.017%

Electrolyte solutions

Preparation of 1M HCl solution takes place by diluting 89 ml of 11.3 N AR-grade HCl to 1000 ml using double distilled water.

Preparation of inhibitor solutions

The inhibitor stock solution was of 1000 ppm of 1-isonicotinoyl-4-pyridin-2-yl Piperazine (ICPP) was prepared by dissolving 2.68 gm of ICPP respectively in 1 litre of 1 M hydrochloric acid and it was diluted to 100, 200, 300, 400, 500, 600, 700, 800 and 900 ppm. These diluted solutions were used as a corrosion inhibitor for further studies.

Weight loss studies

For weight loss measurements, mild steel specimens were cut into a size of 5cm X 1cm X 0.1 cm. Emery papers ranging from 110 to 410 grades. This mild steel specimen was pickled using pickling solution for used to clean. The surface of specimens and degreased with trichloroethylene, washed with double distilled water, and finally dried. Dried specimens were stored in a vacuum desiccator containing silica gel. After cleaning, mild steel specimen was weighed and completely immersed in the solution by hanging from the glass rod using teflon thread for different temperatures (303, 313, 323 and 333 K) with and without inhibitor at 1 h. From the weight loss measurements, corrosion rate,⁶ inhibition efficiency (IE) and surface coverage (θ) were calculated by the following equations.

$$\text{Corrosion rate (CR)} = \frac{8.76 \times 10,000W}{ATD}$$

Where T = time of exposure in hr; W = weight loss of test specimen in g; A = area of test specimen in cm², D = density of material in gcm⁻³, CR = corrosion rate in mmpy.

$$\text{Inhibition efficiency (\%IE)} = \frac{W_b - W_{(Inh)}}{W_b} \times 100$$

$$\text{Surface coverage } (\theta) = \frac{W_b - W_{(Inh)}}{W_b}$$

Where W_b and $W_{(i)}$ are the corrosion rates of mild steel in the without and with of inhibitor respectively at the same temperature.

EVALUATION OF THERMODYNAMIC PARAMETERS

Activation parameters

Activation parameters such as enthalpy of activation (ΔH), entropy of activation (ΔS) and activation energy (E_a) were calculated using Arrhenius equation and the transition state equation⁷

$$\text{Log CR} = \frac{-E_a}{2.303RT} + \log A$$

Where R is the universal gas constant ($8.314 \text{ JK}^{-1}\text{mol}^{-1}$), T is the absolute temperature (K) and A is the Arrhenius pre-exponential factor.

$$\text{CR} = \frac{RT}{Nh} \exp\left(\frac{\Delta S^\circ}{R}\right) \exp\left(\frac{\Delta H^\circ}{RT}\right)$$

Where, h is planck's constant and N is the Avogadro number, ΔH° is the change in enthalpy of activation and ΔS° is the change in entropy of activation.

The plots of $\log \text{CR}$ versus $1000/T$ and $\log(\text{CR}/T)$ versus $1000/T$ are giving a straight line with a slope of $-E_a/RT$ and $(-\Delta H^\circ/R)$ and intercept of A and $[\ln(R/Nh) + (\Delta S^\circ/R)]$ respectively. Activation parameter calculation was carried out using the slope and intercepts of the Arrhenius plot and transition plot.

Adsorption parameters

Adsorption parameters such as the enthalpy of adsorption (ΔH_{ads}), free energy of adsorption (ΔG_{ads}) and entropy of adsorption (ΔS_{ads}) were calculated by Langmuir adsorption isotherm, that is presented by equation.

$$\frac{C_{\text{inh}}}{\theta} = \frac{1}{K_{\text{ads}}} + C_{\text{inh}}$$

Where C_{inh} is the inhibitors concentration, K_{ads} is equilibrium constant, θ is surface coverage.

$$\log \frac{\theta}{1-\theta} = \log A + \log C_{\text{inh}} - \frac{Q_{\text{ads}}}{2.303RT}$$

Where A is a constant, Q_{ads} is the heat of adsorption or enthalpy of adsorption.

Equilibrium constant K_{ads} was calculated by the intercepts ($1/K_{\text{ads}}$) of the straight line that was obtained from the plot of C_{inh}/θ Vs C_{inh} . For calculating the free energy of adsorption, the equilibrium constant value was substituted in the equation.

$$\Delta G_{\text{ads}} = -RT \ln (55.5K_{\text{ads}})$$

The plot of $\log(\theta/1-\theta)$ Vs $1000/T$ at various inhibitor concentrations give a straight line, whose slope is $-\Delta H_{\text{ads}}/2.303R$ (R). Calculation of enthalpy of activation ΔH_{ads} was carried out using the slope value. The entropy of activation (ΔS_{ads}) is given by the equation.

$$\Delta G_{\text{ads}} = \Delta H_{\text{ads}} - T\Delta S_{\text{ads}}$$

Weight loss measurements

The value of inhibition efficiency, surface coverage and corrosion rate for the various concentrations of inhibitor in 1M HCl for a period of 1 h at various temperatures are summarized in Table 1. The inhibition efficiency increases initially with increasing concentration of inhibitor and at a later stage, there is a decreasing trend. This result shows that inhibition efficiency decreased with increase in temperature given figure 4. This may be due to the fact that the inhibitive film formed on the metal surface was protective in nature at high temperature because of desorption of the inhibitor molecules on the metal surface⁸. The maximum inhibition efficiency of the compound was found to be 95.42% in 1M HCl for 900 ppm of ICPP at 303 K.

Table 1: Inhibition efficiency of ICPP mild steel in acid medium at 303K-333K

Conc. of ICPP (ppm)	Corrosion rate (mmpy)	Inhibition efficiency (%)	Corrosion rate (mmpy)	Inhibition efficiency (%)	Corrosion rate (mmpy)	Inhibition efficiency (%)	Corrosion rate (mmpy)	Inhibition efficiency (%)
Blank	121.85	-	158.01	-	572.09	-	961.92	-
100	12.72	89.56	37.64	76.18	156.45	72.65	305.24	68.27
200	10.26	91.58	32.13	79.66	132.94	76.76	269.90	71.94
300	8.33	93.16	29.16	81.54	118.13	79.35	241.11	74.93
400	8.10	93.35	29.08	81.59	110.40	80.70	224.74	76.64
500	7.58	93.77	24.03	84.79	102.29	82.12	220.50	77.08
600	7.51	93.83	22.69	85.64	95.00	83.39	184.79	80.79
700	6.62	94.57	21.79	86.21	88.45	84.54	177.72	81.52
800	5.72	95.30	20.16	87.24	85.40	85.07	163.44	83.01
900	5.58	95.42	16.14	89.78	70.22	87.72	144.47	84.98

FT-IR spectral analysis

FT-IR spectrum of mild steel in 1M HCl, ICPP and mild steel in 1M HCl with the inhibitor immersed ICPP are shown in figure 1, 2 and 3. The peak values obtained from FT-IR spectrum are

summarized in Table 2. The barrier film formation is due to the interaction of nitrogen, oxygen atoms present in ICPP with Fe in mild steel there by Fe-ICPP complex was formed. It prevents the corrosion process. The peaks between 400 and 700 cm^{-1} are mainly due to Fe_2O_3 .

Table 2: FT-IR Peak Value (cm⁻¹) of ICPP and Mild steel in 1M HCl and Mild steel in 1N HCl with inhibitor (ICPP)

S.no	Mild steel in 1M HCl (cm ⁻¹)	ICPP (cm ⁻¹)	Mild steel in 1M HCl with ICPP(cm ⁻¹)	Possible groups
1	3432.28	-	-	OH
2	-	3418.49	3434.53	N-H stretch
3	-	2843.95	2831.05	O-H stretch
4	2829.8 1592.98	-	-	δHOH
5	-	2220.4	2264.09	C=N in aromatic ring
6	-	1636.14	1599.76	C=O attached to aromatic ring
7	-	1436.94	1385.83	C=C stretch
8	-	1242.65	1309.98	C-C-N bending
9	1358.13	-	-	δOH
10	-	1161.28	1111.72	cyclohexane ring vibration
11	773.95	-	-	γOH
12	-	784.52	-	-C-H out of plane bending
13	561.02	-	-	γFeO

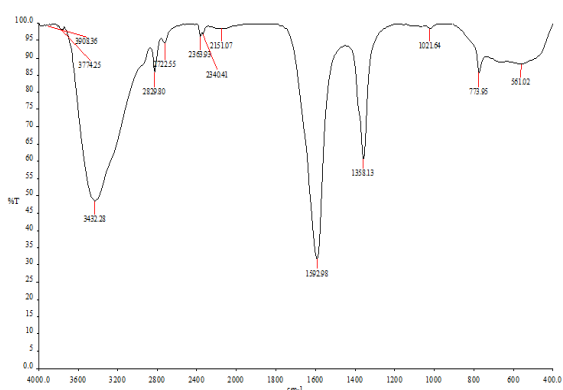


Figure 1: FT-IR spectrum of mild steel in 1M HCl

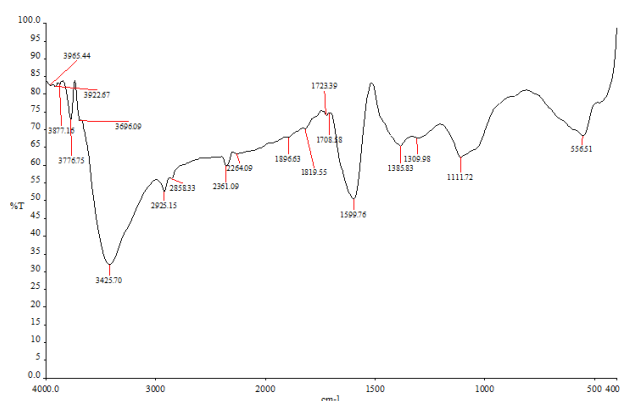


Figure 2: FT-IR spectrum of ICPP

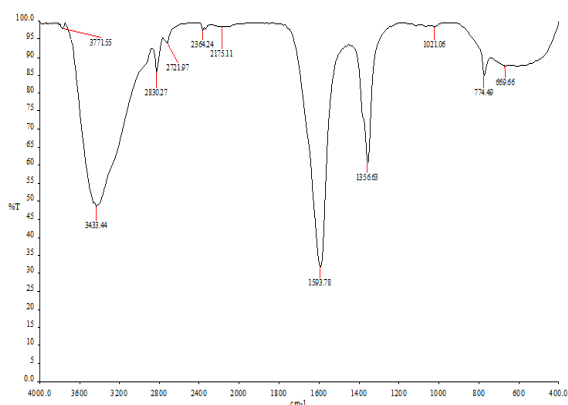


Figure 3: FT-IR spectrum of mild steel in 1N HCl

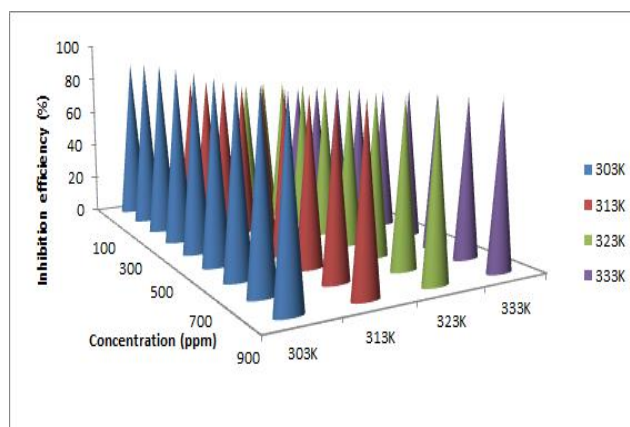


Figure 4: Temperature studies 1M HCl with ICPP

Thermodynamic and activation parameters

The Arrhenius and transition state plots are given in Figure 5 and 6. The calculated values of activation energy (E_a), enthalpy of activation (ΔH[‡]), the entropy of activation (ΔS[‡]) are presented in Table 3.

Table 3: Thermodynamic parameters of mild steel corrosion with ICPP

Conc of ICPP (ppm)	Activation energy (KJ mol ⁻¹) (Ea)	Enthalpy (KJ mol ⁻¹) (ΔH°)	Entropy (J mol ⁻¹ K ⁻¹) (ΔS°)
Blank	62.61	113.09	-182.35
100	86.44	168.69	-178.16
200	88.71	170.61	-177.99
300	96.33	177.30	-177.54
400	101.86	185.40	-176.88
500	105.93	200.43	-175.63
600	107.96	208.80	-174.80
700	110.67	213.03	-174.72
800	113.72	222.02	-173.90
900	117.79	229.00	-173.27

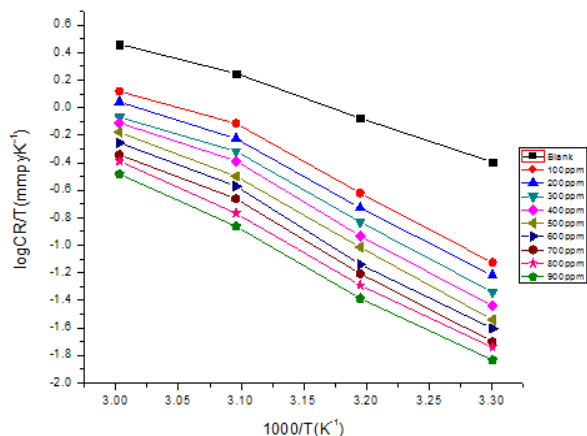


Figure 5: Arrhenius plots for absence and presence of ICPP

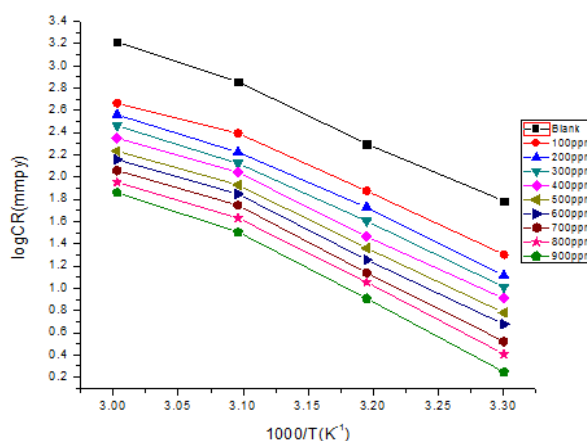


Figure 6: Transition state plots for absence and presence of ICPP

It could be seen that Ea is lowest (62.61 KJ mol⁻¹) for the free acid solution but higher (117.79 KJ mol⁻¹) in the presence of the ICPP at 900 ppm, with Ea values increasing as the concentration of the inhibitor increases. The increase in Ea with concentration is associated with an increase in energy barrier for the mild steel corrosion and is dependent on the concentration of the inhibitor. The value of ΔH° positive indicating the endothermic nature of the corrosion process for the formation step of the activated complex. On the other hand, the negative values of ΔS° in the

absence and presence of the ICPP indicating that the formation of activated complex from reactant represent an association step rather than dissociation step, meaning that a decrease in disordering takes place in going from reactants to the activated complex^{9,10}. The values of Ea and ΔH° are (Figure 7) higher in the presence of the inhibitor. This result shows that the energy barrier of the corrosion reaction is increased without changing the mechanism of dissolution.

Table 4: Adsorption parameters of mild steel corrosion with ICPP

Conc of ICPP (ppm)	-(ΔG) KJ/mole			
	303 K	313 K	323 K	333 K
100	23.83	22.49	22.24	22.03
200	24.02	22.58	22.53	22.14
300	24.12	22.61	22.59	22.37
400	24.24	22.77	22.67	22.42
500	24.50	22.92	22.89	22.70
600	24.88	23.38	23.32	22.72
700	25.53	23.86	23.82	23.44
800	25.98	24.56	24.50	24.18
900	27.13	25.99	25.78	25.46

When Ea is higher the reaction is slow and very sensitive to temperature. The increase in the activation energy in the presence of inhibitors signifies physical adsorption¹¹. The adsorption process becomes spontaneous and adsorbed layer of mild steel becomes stable when ΔG°_{ads} are negative and the absolute ΔG°_{ads} value decreases because the stability of adsorption layer is inversely proportional to a temperature which there by confirms the physical adsorption. The Gibbs free energy of adsorption (ΔG°_{ads}) calculated from surface coverage (θ) is listed in Table 4.

Adsorption parameters and isotherms

The adsorption isotherm was useful to investigate the interaction between the ICPP and the mild steel surface in 1M HCl were calculated from the thermodynamic equation over the temperature range 303 K to 333 K. A Plotting C_{inh} / θ Vs C_{inh} respectively (Figure 8) resulted in a straight line, which indicates that the inhibitor adsorption obeys the Langmuir adsorption isotherm, on the metal surface, forming a strong protective barrier film which prevented the direct and indirect

contact with the metal-containing acid. The adsorption process becomes spontaneous and adsorbed layer of mild steel becomes stable when ΔG°_{ads} is negative and the absolute ΔG°_{ads} value decreases because the stability of adsorption layer is inversely proportional to a temperature which there by confirms the physical adsorption. Based on the data presented in Table 4. The negative value of ΔG°_{ads} ranging from -27.13 to -25.46 KJ/mol indicated that the values of ΔG°_{ads} negative sign are usually characteristic of a strong interaction and a high efficient

adsorption. Generally, values of ΔG°_{ads} around -20 KJ mol⁻¹ or lower negative are consistent with the electrostatic interaction among the charged metal and the charged molecules (physisorption). Whereas, the more negative values greater than -40 KJ mol⁻¹ involve charge sharing or transfer from the inhibitor to the surface of the metal to form a co-ordinate type of bond (chemisorption)¹². Calculated ΔG°_{ads} values indicate that the adsorption mechanism of the synthesized inhibitor on mild steel in 1M HCl solution is physical adsorption.

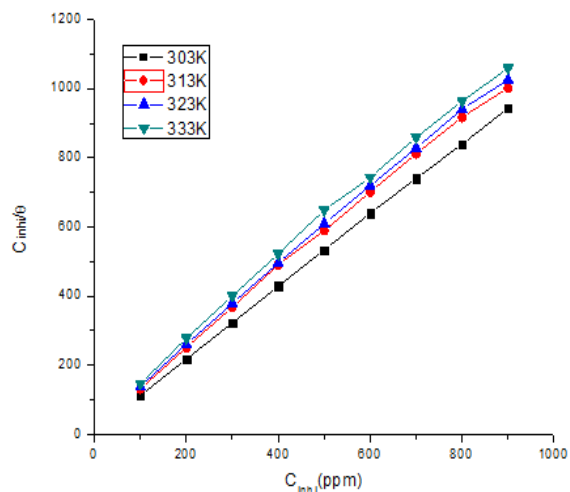


Figure 7: Adsorption relation

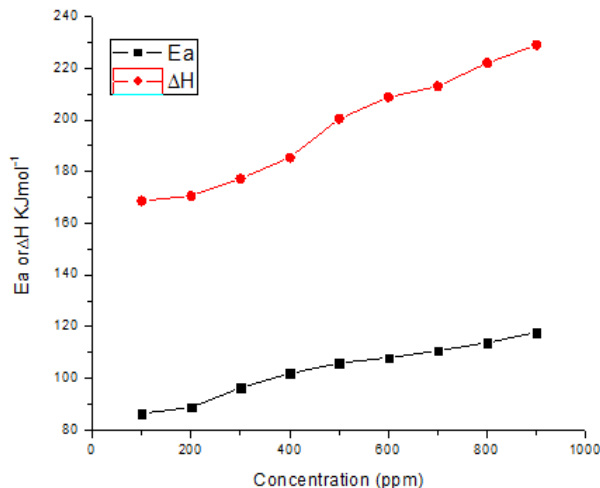


Figure 8: Langmuir adsorption isotherm

Table 5: Adsorption factors for ICPP at different temperatures

Temperature (K)	R ²	slope	K _{ads}	-ΔG
303	0.9999	1.139	4772	23.45
313	0.9985	1.197	2757	22.93
323	0.9988	1.119	2519	21.68
333	0.9978	1.141	1852	20.15

Figure 8 shows a plot of C/θ versus C for various temperatures and the values of R^2 and slope are listed in the Table 5 which is used to describe the adsorption process that is based on assumption already discussed. The values of ΔG°_{ads} was calculated by equation 3.3 The values are given in the table, then the value at 303 K was found to be -23.45 KJ/mol. which indicates that the ICPP is strongly adsorbed on the surface of the mild steel. From the table, it can be observed that the ICPP shows that the ΔG°_{ads} value and less negative than -40 KJ/mol at all temperatures, the physical adsorption contributes to a higher percentage of ICPP adsorption on the mild steel surface. The

value of K_{ads} and ΔG decreases with increasing in temperature¹³.

Atomic Force Microscopy (AFM)

AFM is a dynamic tool to examine the surface morphology to study the nature of protective layer formed on the surface of the mild steel. The 2D and 3D AFM images were taken at room temperature in the first position range of 0.05 μm to 0.65 μm, second position range of 0.05 μm to 0.90 μm and the average roughness of mild steel surface in 1 M HCl solution as shown in Figure 9A & B

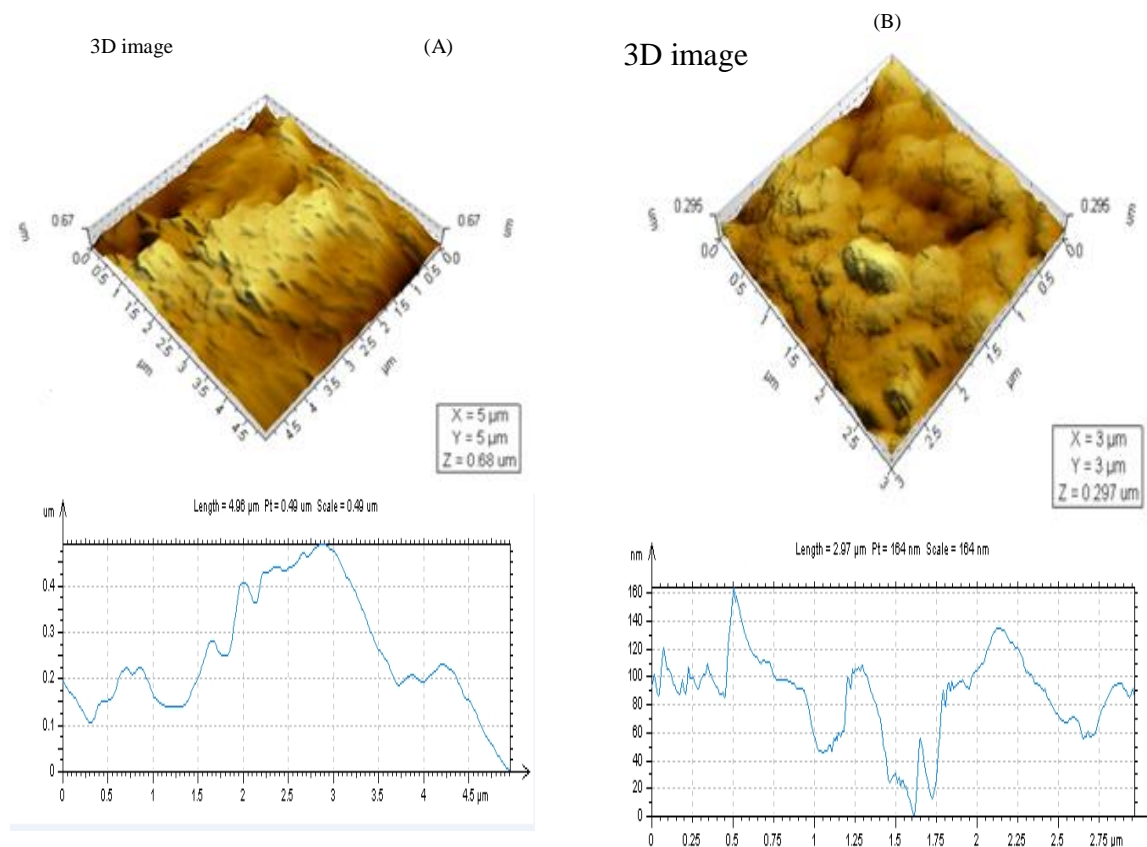


Figure 9A & B: AFM images of mild steel in 1M HCl with ICPP

The mild steel surface is severely damaged due to acid attack are clearly evident in the photograph. However, in presence of an optimum concentration of ICPP of 900 ppm the average roughness is reduced to the position from 0.025 μm to 0.27 μm as shown in Figure 9A & B which shows that the formation of the protective film of Fe-ICPP on the metal surface there by inhibiting the corrosion of mild steel¹⁴. From the results, it is clear that the inhibition of mild steel corrosion in the presence of inhibitor is mainly due to the formation of a protective layer by

adsorption of inhibitor molecules over the surface of the mild steel. AFM data for mild steel is given in Table 6. The results obtained from AFM and FT-IR suggest that the mechanism of inhibition is occurring mainly through the adsorption process. The adsorption of the inhibitors obey Langmuir's adsorption isotherm. The less negative value of ΔG_{ads} indicates the spontaneous and physical adsorption of the inhibitors on the metal surface.

Table 6: AFM parameters for mild steel with ICPP

Sample	Root mean Square roughness (μm)	Average roughness (μm)	Maximum peak height (μm)	Maximum surface height (μm)
1M HCl without ICPP	0.1290	0.1070	0.305	0.680
1M HCl with ICPP	0.0437	0.0341	0.148	0.297

REFERENCES

- Singh DDN, Singh TB, Gaur B. The role of the metal cations in improving the inhibitive performance of hexamine on the corrosion of steel in hydrochloric acid solution. *Corrosion Science* 1995; 37:1005-1019.
- Yadav M, Behera D, Sharma U. Corrosion protection of N 80 steel in hydrochloric acid by substituted aminoacids. *Corrosion Engineering Science Technology* 2013; 48:19-27.
- Yadav M, Behera D, Sharma U. Non toxic corrosion inhibitors for N 80 steel in hydrochloric acid. *Arabian Journal of Chemistry*. doi:10.1016/j.arabjc. 2012. 03. 011
- Yadav M, Sharma U. Eco-friendly corrosion inhibitors for N 80 steel in hydrochloric acid . *Journal of Material and Environmental Science* 2011; 2:407-414.
- Yadav M, Kumar S, Sharma D. Experimental and quantum chemical studies on corrosion inhibition effect of synthesized organic compounds on N 80 steel in hydrochloric acid. *Industrial Engineering. Chemistry Research* 2013; 52:14019-14029.
- Deng Q, Shi HW, Ding NN, Chen BQ, He XP, Liu G, Tang Y, Long YT, Chen GR. Novel trizolybis-amino acid derivatives readily synthesized via click chemistry as potential corrosion inhibitors for mild steel in HCl. *Corrosion Science* 2012;57:220-227.
- Ahmed Y Musa, Abdul amir H. Kadhum, Abu Bekar Mohamad, Abdul Razak Daud, Mohd Sobri Takriff, Siti kartom Kamarudin. A comparative study of the corrosion inhibition of mild steel in sulphuric acid by 4, 4-dimethyloxazolidine-2-thione. *Corrosion Science* 2009; 51:2393-2399.

8. Khaled, KF. Understanding Corrosion Inhibition of Mild Steel in Acid Medium by Some Furan Derivatives: A Comprehensive Overview. *Journal of the Electrochemical Society* 2010; 157(3):116-124.
9. Sumathi Paramasivam, Kannan Kulanthai, Gnanavel Sadhasivam, Rekha Subramani. Corrosion Inhibition of Mild Steel in Hydrochloric Acid using 4-(pyridin-2-yl)-N-p-tolylpiperazine-1-carboxamide. *International Journal of Electrochemical Science* 2016; 11:3393-3414.
10. Mahendra yadav, Sushil kumar, Indra Bahadur, Deresh Ramjugernath. Corrosion inhibitive effect of synthesized thiourea derivatives on mild steel in a 15% HCl solution. *International Journal of Electrochemical Science* 2014; 9:6529-6550.
11. Li X, Deng S, Fu H, Li T. Adsorption and inhibition effect of 6-benzylaminopurine on cold rolled steel in 1.0M HCl. *Electrochimica acta* 2009; 54(16): 4089-4098.
12. Behpour M, Ghoreishi SM, Soltani N, Salavati-Niasari M, Hamadani M, Gandomi, A. Electrochemical and theoretical investigation on the corrosion inhibition of mild steel by thiosalicylaldehyde derivatives in hydrochloric acid solution. *Corrosion Science* 2008; 50(8): 2172-2181.
13. Chandrabhan verma, Quraishi MA, Ebense EE. Electrochemical studies of 2-amino-1, 9-dihydro-9-((2-hydroxy ethoxy) methyl)-6H-purin-6-one as green corrosion inhibitor for mild steel in 1.0 M hydrochloric acid solution. *International Journal of Electrochemical Science* 2013; 8: 7401-7413.
14. Ganapathi Sundaram R, Sundaravadivelu M, Karthik G, Vengatesh G. Inhibition effect of 4-hydroxyquinoline-2-carboxylic acid on corrosion of mild steel in sulphuric acid solution. *Journal of Chemical and Pharmaceutical. Research* 2015; 7: (9) 823-835.

Cite this article as:

Sumathi P, Kannan K. Activation parameters and adsorption behavior of 1-isonicotinoyl-4-pyridin-2-yl piperazine on mild steel in acid environment. *Int. Res. J. Pharm.* 2017;8(4):80-86 <http://dx.doi.org/10.7897/2230-8407.080453>

Source of support: Nil, Conflict of interest: None Declared

Disclaimer: IRJP is solely owned by Moksha Publishing House - A non-profit publishing house, dedicated to publish quality research, while every effort has been taken to verify the accuracy of the content published in our Journal. IRJP cannot accept any responsibility or liability for the site content and articles published. The views expressed in articles by our contributing authors are not necessarily those of IRJP editor or editorial board members.